Lasers in Manufacturing Conference 2023

Black marking of titanium containing commercial glass

Lukas Janos Richter*, Clemens M. Beckmann, Jürgen Ihlemann

Institut für Nanophotonik Göttingen e.V., Göttingen, Germany

Abstract

Laser marking of glass products can be used to enhance the visual appearance, for product identification, traceability and fraud prevention. We demonstrate that high-contrast black markings can be produced on commercial TiO_2-containing glasses by pulsed excimer laser irradiation without any special treatment of the surface. The black markings can be partly attributed to a scattering effect due to the formation of a microstructure on the surface. It is enhanced by laser-induced oxygen reduction of the TiO_2 and an associated increase in light absorption. Measurements show a phase separation in titanium and silicon-rich material in an area of the microstructure close to the surface. An inclination of the sample during irradiation allows the fabrication of microstructures with a preferred direction. Our results show a simple method for creating high-contrast surface markings on commercial glass.

Keywords: TiO_2-containing glass; Black marking; Surface microstructure; Excimer laser

1. Introduction

Laser-based methods for marking the surface of glass are diverse. A standard technique is the marking of various types of glass by CO_2 laser irradiation. A scattering effect on the glass surface leads to a marking effect [Allcock et al., 1995]. Another way of generating markings by laser irradiation can be realized by creating periodic structures in the glass surface. Colored markings can thus be obtained by diffraction effects [Meinertz et al., 2022]. Other methods use, for example, plasmonic effects [Ihlemann et al., 2022] or the burning in of dyes in the glass surface [Altan and Waibel, 2018].

To produce highly refractive glasses, the admixture of TiO_2 is a standard technique. Laser irradiation of TiO_2 has already been investigated. Laser-induced oxygen reduction of TiO_2 and an associated increase in light absorption have been reported [Zheng et al., 2008, Van Overschelde et al., 2007, Sol and Tilley, 2001, Starbova et al., 2008]. Laser irradiation of TiO_2 coatings and TiO_2 containing glasses can also cause phase separation or phase transition [Liu et al., 2008]. The formation of microstructures by pulsed excimer laser irradiation

* Corresponding author. Tel.: +49-551-5035-57

E-mail address: Lukas.richter@ifnano.de

(wavelength λ = 248 nm) has also been reported [Narazaki et al, 2005].

In this work, a method for the production of particularly high-contrast black markings with high resolution on surfaces of glasses containing TiO_2 is presented. The commercial Schott glasses "N-SF11", "SF11" and "N-F2" are treated here. However, the process can also be implemented on other highly refractive TiO_2 containing glasses. The surfaces are processed with pulsed ultraviolet radiation of an ArF excimer laser (λ = 193 nm). The irradiation causes the formation of a scattering microstructure on the glass surface, which is accompanied by a phase separation into a titanium-rich and a silicon-rich phase. The marking effect is enhanced by increased light absorption due to laser-induced oxygen reduction of TiO_2. Element mappings by energy dispersive x-ray (EDX) spectroscopy along the cross-section of a microstructure reveal depth-selective phase separations. By tilting the sample during laser irradiation, a preferred direction can be achieved in the microstructure that is formed.

The production of high-contrast markings on glass surfaces is desired not only for decorative processes, but also for product identification in manufacturing processes or fraud prevention. Since the here presented process does not require the use of additives, it is also of interest for applications where strong requirements on the used materials, like e. g. in medicine and pharmacy, exist.

2. Materials and Methods

Experiments were conducted on three different glass types from Schott: SF11, N-SF11 and N-F2. These respectively have the following TiO_2 weight contents, as determined in a previous work by EDX analysis: 4.8 %, 28 % and 15 % [Richter et al., 2022]. The samples were plates, polished on both surfaces. Laser irradiation was performed with an ArF excimer laser (Lambda Physik LPXpro, $\lambda = 193$ nm, pulse duration 20 ns). A mask projection setup was used, as shown in figure 1 (a). With a demagnification of about 10:1, a rectangular mask was imaged onto the sample through a spherical fused silica lens of 100 mm focal length. A homogenous part of the laser beam was selected by the rectangular mask with an aperture of 2 – 5 mm. A variable attenuator allows the variation of the fluence. The fluence was determined by measuring the laser pulse energy in the sample position and the spot size of the irradiated area. The samples were mounted so that the tilt was adjustable. Therefore, the angle of laser light incidence on the sample "φ" can be varied as shown in figure 1 (b). Prior to analysis, the samples were cleaned with a KOH solution in an ultrasonic bath (Deconex 15PF-x in water (1:2) for 10 min at 50 °C).

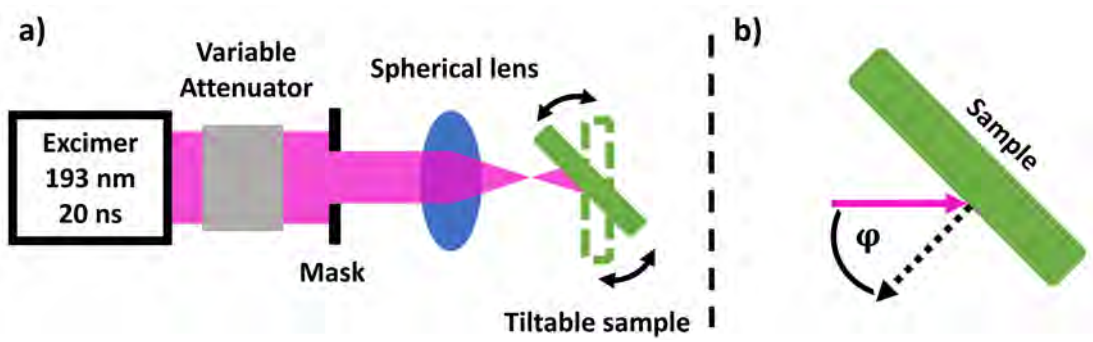

Fig. 1. Schematic sketch of the laser setup. In part (a) the laser beam path is shown: The excimer-laser light traverses a variable attenuator. A transparent mask area is then imaged on the samples by a spherical lens. The sample is mounted in a holder so that an inclination can be selected. "φ" is defined as the angle between the incident laser light and the surface normal of the sample, as shown in part (b).

A surface analysis of the samples was performed using an optical microscope (Zeiss, Imager.Z2m). More detailed surface analyses were conducted with a scanning electron microscope (SEM; Zeiss, EVO MA10) and combined material analyses by EDX spectroscopy (Bruker Quantax system with an XFlash 410-M detector at 20 kV acceleration voltage of the incident electrons).

3. Results

Laser irradiation of the TiO_2-containing glasses within a fluence range of approximately 200 - 400 $\mathrm{mJ/cm^2}$ leads to the formation of a microstructure. Laser irradiation below this fluence range does not lead to any significant material modification, whereas laser irradiation above this fluence range results in a smooth ablation of the material. The formation of the microstructure becomes visible as a bumpy structure from roughly 50 laser pulses on. With the application of further laser pulses, the bumpy structure intensifies and connects to form a random oriented hill-like structure with valleys. A more detailed description of this structure formation with the pulse number has already been published [Richter et al., 2022]. The "period" is between 2 - 5 µm, increasing with increasing laser pulse number. The height of the structure is a few µm, with the height also increasing with increasing pulse number. Two examples of such microstructures can be seen in SEM images in figure 2. In part (a) SF11 glass was irradiated with 1000 laser pulses at 300 $\mathrm{mJ/cm^2}$ at normal incidence (φ = 0°). The hill-valley like structure with a period of some µm is clearly visible. In part (b) N-F2 glass was irradiated with 1000 laser pulses at 260 $\mathrm{mJ/cm^2}$ at normal incidence (φ = 0°). The angle of observation is 45°, therefore the structure height is visible, being in the same range as the structure period.

Along with microstructure formation, phase separation of the material occurs. This is visible in element mappings by EDX, as shown in figure 3. In part (a) a SEM image of SF11 glass irradiated with 1000 laser pulses at a fluence of 300 $\mathrm{mJ/cm^2}$ at normal incidence (φ = 0°) is shown. The corresponding EDX analysis in part (b) clearly shows a phase separation between a titanium-rich phase (red) on the hills and silicon-rich phase (green) on the slopes. The phase separation also occurs at glasses with other TiO_2 contents, as can be seen in part (c) and (d) on N-SF11 glass after irradiation with 1000 laser pulses at 250 $\mathrm{mJ/cm^2}$ at normal incidence (φ = 0°).

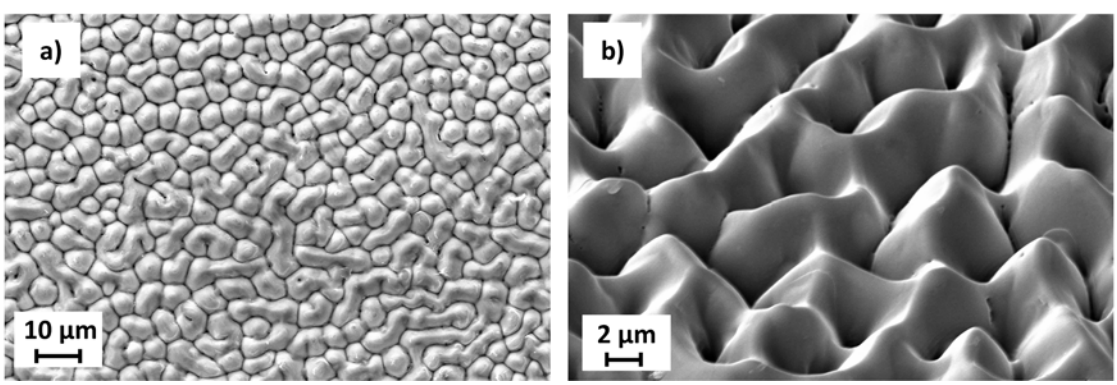

Fig. 2. SEM images of laser irradiated samples ($\lambda = 193\ \mathrm{nm}$) showing the surface microstructure. In image (a) SF11 glass was irradiated with 1000 laser pulses using a fluence of 300 $\mathrm{mJ/cm^2}$ at normal incidence (φ = 0°). Image (b) shows the surface of N-F2 glass at an angle of observation of 45° after 1000 laser pulses with a fluence of 260 $\mathrm{mJ/cm^2}$ at normal incidence (φ = 0°).

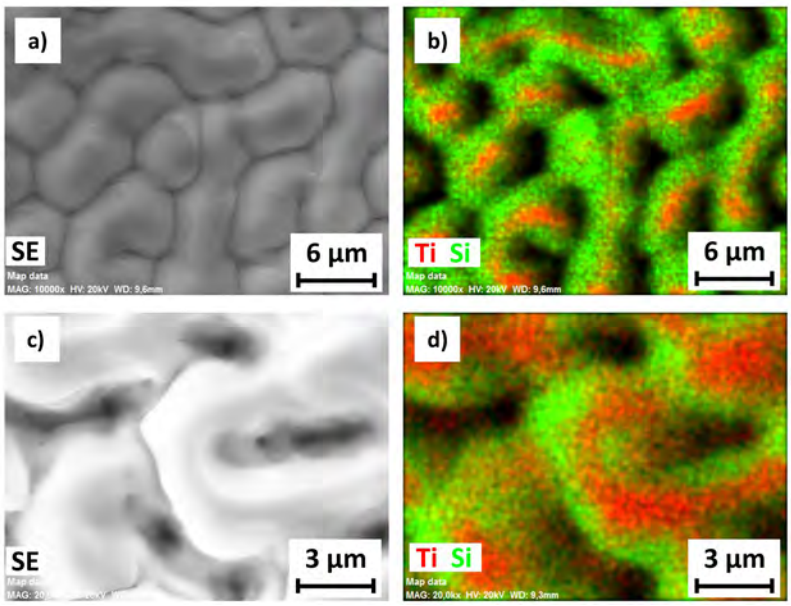

Fig. 3. SEM and corresponding element mappings by EDX (Ti: red, Si: green) of the irradiated surfaces. Image (a) shows the surface microstructure of SF11 glass after 1000 laser pulses ($\lambda = 193\ \mathrm{nm}$) using a fluence of 300 $\mathrm{mJ/cm^2}$ at normal incidence (φ = 0°). The corresponding false-color image in (b) shows the separation in a titanium-rich and a silicon-rich phase. Image (c) shows a surface microstructure on N-SF11 glass fabricated with 1000 laser pulses ($\lambda = 193\ \mathrm{nm}$) using a fluence of 250 $\mathrm{mJ/cm^2}$ at normal incidence (φ = 0°). In (d) the corresponding element mapping is depicted.

To further investigate the laser-induced phase separation, the glass sample was divided by a clear fracture. The cross-sectional area of the fracture can be seen in the SEM images in figure 4. In part (a), the surface structure on N-SF11 glass formed by laser irradiation with 1000 laser pulses at a fluence of 300 $\mathrm{mJ/cm^2}$ at normal incidence (φ = 0°) is visible in the upper part of the image. The angle of observation is approximately perpendicular to the cross-sectional area. The fracture edge in the glass is horizontally located in the center of the image. It can be seen that a smooth cross-sectional area and fracture edge has formed without affecting the surface structure. Image (b) shows an element mapping by EDX of the corresponding area (Ti: red, Si: green). Image (c) shows a higher magnification image of a hill of the surface structure at the cross-sectional area of the fracture. Image (d) shows the corresponding element mapping. A phase separation is clearly visible. The hills are rich in titanium, while the underlying glass has a mixed phase between titanium and silicon, as is the case with the untreated glass. A structure height of about 2 µm can be measured.

In addition to the phase separation, there is an oxygen reduction of the TiO_2 on the hills. This has been shown by Raman spectroscopy in our previous work [Richter et al., 2022]. An oxygen reduced titanium-rich phase thus forms on the hills. It is known in the literature that oxygen reduced titanium oxides exhibit increased light absorption [Zheng et al., 2008]. This effect, in combination with the strong light scattering by the microstructure on the surface, enables the generation of high-contrast markings by the laser irradiation. Figure 5 shows an example of such a marking. Here, N-SF11 glass was irradiated with 200 laser pulses at a fluence of 300 $\mathrm{mJ/cm^2}$ at normal incidence (φ = 0°). Individual pixels combine to form a QR code as can be seen in the camera image in part (a). In part (b), a microscope image of the high-contrast square pixels is

visible. In part (c), a microscope image with high magnification is visible. Here, the microstructure of the surface is visible.

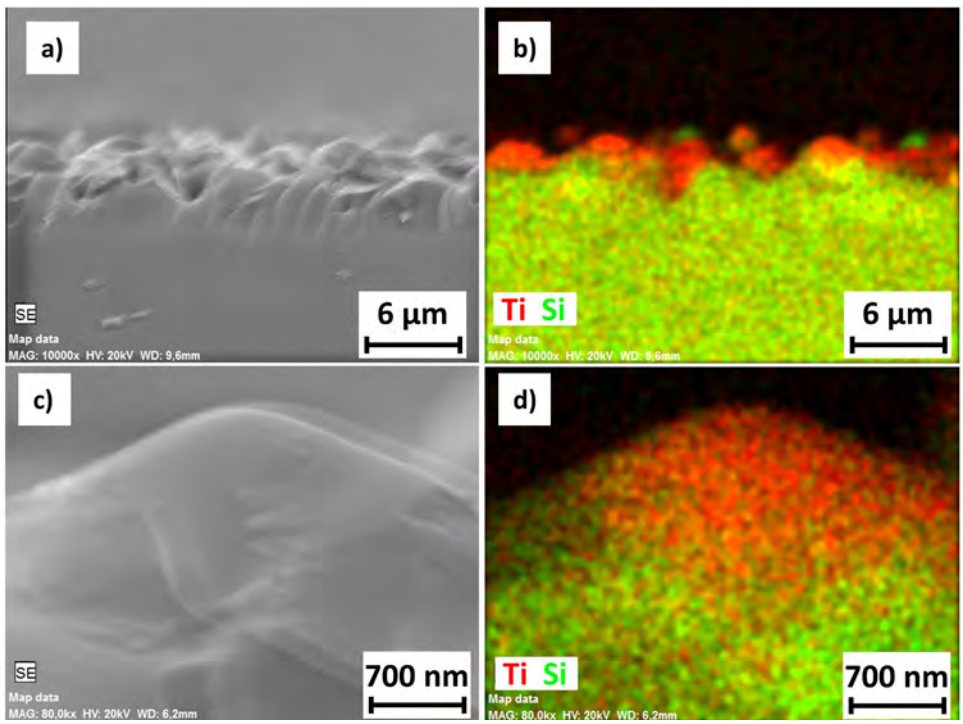

Fig. 4. SEM images and element mappings of the cross-sectional area of a N-SF11 glass sample. The glass surface was irradiated using a laser wavelength of $\lambda = 193\ \mathrm{nm}$ with 1000 laser pulses at a fluence of 300 $\mathrm{mJ/cm^2}$ at normal incidence of the laser light (φ = 0°). In the upper part of image (a), the surface structure can be seen. In the center of the image, the fracture edge runs horizontally, so that the cross-sectional area of the fracture can be seen. Part (b) shows the element mapping of the corresponding area (Si: red, Ti: green). Part (c) shows an enlarged area of a hill of the laterally viewed surface structure at the fracture surface. Part (d) shows the corresponding element mapping.

Further experiments show that the microstructure formation can be influenced by additional parameters. Irradiation of the sample at an angle (0° > φ > 90°, cf. figure 1 (b)), will result in an orientation of the microstructure. Figure 6 shows microscope images of N-SF11 glass laser irradiated at 300 $\mathrm{mJ/cm^2}$ at an angle of incidence of the laser light of φ = 45°. SEM images of the same sample are shown in figure 7. The number of laser pulses was varied and is indicated in the images. It can be seen that, similar to irradiation under normal incidence, a hill-like structure is formed after 20 to 50 pulses. However, when further laser pulses are applied, a preferred direction of the structure is formed. The hills grow parallel to the direction of laser irradiation, as marked by the pink arrows in the figures. This does not result in the formation of a randomly oriented micronetwork, but in a kind of line structure. As the number of pulses increases, the length of these individual lines increases from about 2 µm to 5 µm.

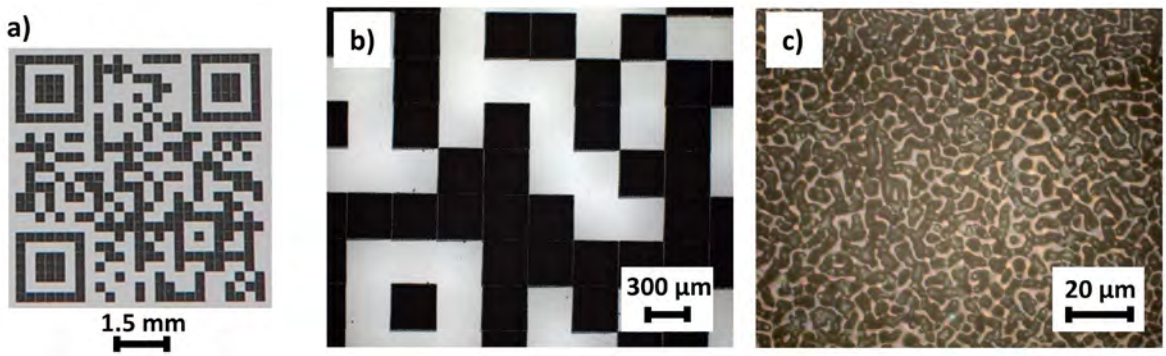

Fig. 5. Black marking as a QR-code fabricated on N-SF11 glass by laser irradiation ($\lambda = 193$ nm) using 200 pulses/pixel with a fluence of 300 $\mathrm{mJ/cm^2}$ at normal incidence (φ = 0°). Image (a) shows a photo of the QR-code. Image (b) and (c) show reflective light microscope images of the sample at different magnifications

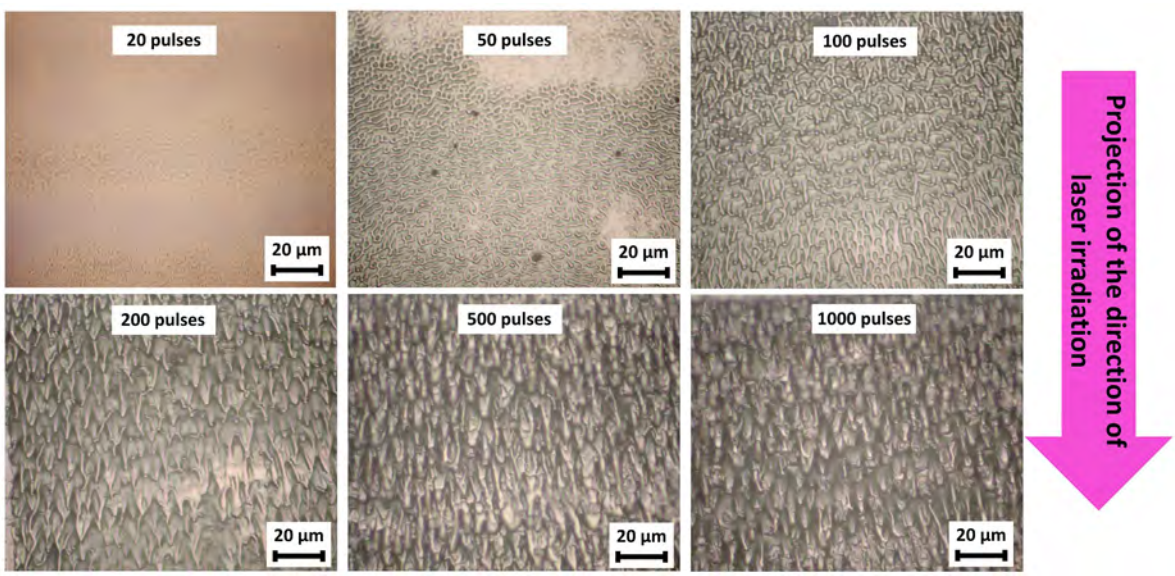

Fig. 6. Brightfield microscope images of N-SF11 glass laser irradiated at an angle of incidence of φ = 45° using a laser wavelength of $\lambda = 193$ nm at a fluence of 300 $\mathrm{mJ/cm^2}$. The laser pulse number is indicated in each image. The projection on the surface of the direction of the laser light is indicated by the pink arrow.

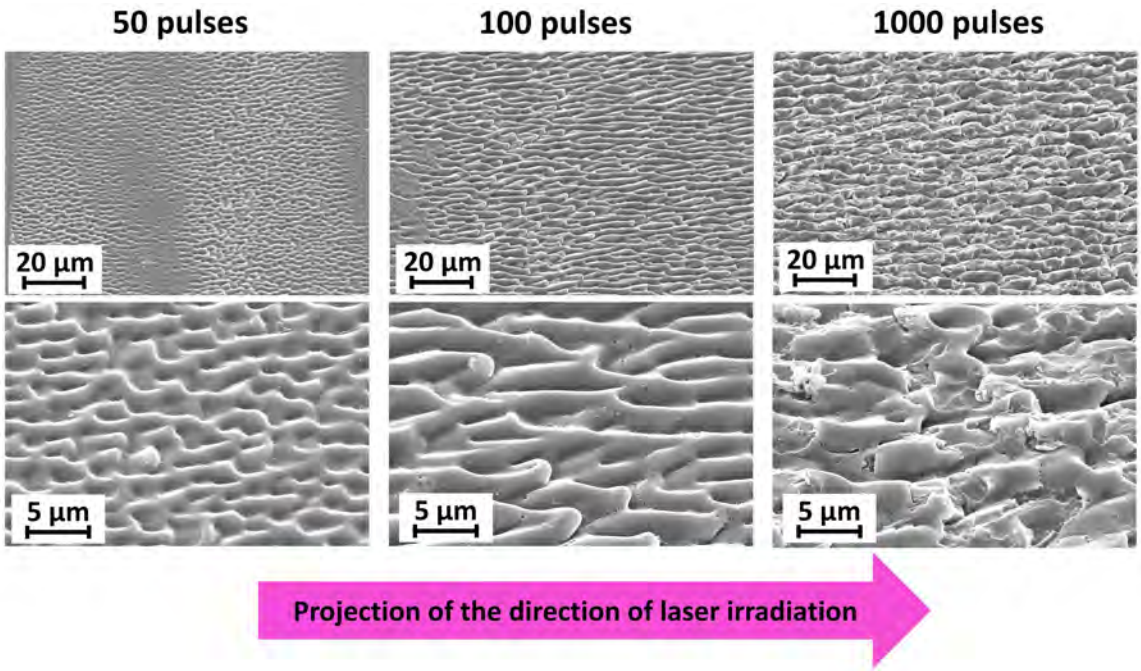

Fig. 7. SEM images of the surface of N-SF11 glass laser irradiated using a laser wavelength of $\lambda = 193\ \mathrm{nm}$ at a fluence of 300 $\mathrm{mJ/cm^2}$ at an angle of incidence of φ = 45° to the glass surface. The laser pulse number is indicated, two magnifications are shown for each pulse number. The projection on the surface of the direction of the laser light is indicated by the pink arrow.

4. Discussion

The process of microstructure formation has already been described in more detail in previous publications [Narazaki et al, 2005, Richter et al., 2022]. In summary, the heating of the material by laser irradiation leads to the formation of a binary composition of TiO_2-SiO_2 mixture. During cooling, preferential evaporation of the SiO_2 occurs, resulting in titanium-rich hill formation. The repeated process through many laser pulses results in the formation of the micro network.

SEM and EDX analyses at the cross-sectional area of the fracture of the glass presented here show that the formation of the titanium-rich phase is confined to a region near the surface. Below this modified region, material compositions are measured as in the non-irradiated region. The oxygen reduction of TiO_2 by laser irradiation has been reported in the literature [Zheng et al., 2008]. The increased light absorption by oxygen reduction and the scattering effect of the microstructure enable fabrication of high-contrast markings on the glass surface.

Laser irradiation of an inclined sample results in the formation of a preferred direction of the microstructure, so that a kind of line structure results. With a few laser pulses, a hill-like structure initially forms, as with laser irradiation under normal incidence. With further laser pulses, these hills then form into lines that grow parallel to the direction of the laser irradiation. A possible explanation is a shadowing effect caused by the hill structures. Areas that lie behind the hill from the point of view of the laser beam are in shadow. Due to the shadowing effect, the material in the shaded regions experiences reduced or no laser energy, resulting in limited or no material modification. In contrast, the areas exposed to direct laser irradiation undergo significant material changes. This discrepancy in energy absorption and material modification between the shadowed and exposed regions leads to the formation of a preferred direction in

the microstructure. Similar observations have been described in the literature on polyethersulfone by XeCl excimer laser irradiation [Niino et al., 1989] and on polyethylene-terephtalate (PET) by ArF excimer laser irradiation [Hopp et al., 1996].

5. Conclusion

In summary, pulsed laser irradiation ($\lambda = 193\ \mathrm{nm}$) of TiO_2 containing glasses leads to randomly oriented microstructure formation accompanied by oxygen reduction of TiO_2. The microstructure exhibits phase separation into a titanium-rich phase on the hills and a silicon rich phase in the valleys. Measurements on the cross section of the structure show material modification close to the surface. Critical parameters in the process are the laser fluence, the number of laser pulses and the TiO_2 content of the glass. A preferred direction of the microstructure can be generated by tilting the sample during laser irradiation. The microstructure and oxygen reduction enable the fabrication of high-contrast markings on commercially available TiO_2 containing glasses.

Acknowledgements

We are grateful to Jens Oltmanns for his help in creating a smooth break in the glass samples.

References

Allcock, G., Dyer, P. E., Elliner, G., Snelling, H. V., 1995. Experimental observations and analysis of CO_2 laser-induced microcracking of glass, Journal of Applied Physics 78, p. 7295

Altan, L. and Waibel, G., 2018. New process of tempering color printed glass by using laser irradiation, Procedia CRIP 74, p. 390

Hopp, B., Csete, M., Révész, K., Vinkó, J., Bor, Z., 1996. Formation of the surface structure of polyethylene-terephtalate (PET) due to ArF excimer laser ablation, Applied Surface Science 96-98, p. 611

Ihlemann, J., Richter, L. J., Meinertz, J., Wunderlich, J., Schindler, N., Günther, A., Oberleiter, B., Rainer, T., 2022. Glass marking by laser transfer implantation (LTI) of plasmonic nanoparticles, Optics and Laser Technology 155, p. 108371

Liu, Y., Zhu, B., Wang, L., Dai, Y., Ma, H., Lakshminarayana, G., Qiu, J., 2008. Femtosecond laser direct writing of TiO_2 crystalline patterns in glass, Applied Physics B 93, p. 613

Meinertz, J., Gödecke, A., Richter, L. J., Ihlemann, J., 2022. Fast fabrication of diffractive patterns on glass by excimer laser ablation, Optics & Laser Technology 152, p. 108148

Narazaki, A., Kawaguchi, Y., Niino, H., Shojiya, M., Koyo, H., Tsunetomo, K., 2005. Formation of a TiO_2 micronetwork on a UV-absorbing SiO_2-based glass surface by excimer laser irradiation, Chemistry of Materials 17, p. 6651

Niino, H., Nakano, M., Nagano, S., Yabe, A., Miki, T., 1989. Periodic morphological modification developed on the surface of polyethersulfone by XeCl excimer laser photoablation, Applied Physics Letters 55, p. 510

Richter, L. J., Beckmann, C. M., Ihlemann, J., 2022. UV laser generated micro structured black surface on commercial TiO_2-containing glass, Applied Surface Science 601, p. 154231

Sol, C. and Tilley, R. J. D., 2001. Ultraviolet laser irradiation induced chemical reactions of some metal oxides, Journal of Materials Chemistry 11, p. 815

Starbova, K., Yordanova, V., Nihtianova, D., Hintz, W., Tomas, J., Starbov, N., 2008. Excimer laser processing as a tool for photocatalytic design of sol-gel TiO_2 thin films, Applied Surface Science 254, p. 4044

Van Overschelde, O., Snyders, R., Wautelet, M., 2007. Crystallisation of TiO_2 thin films induced by excimer laser irradiation, Applied Surface Science 254, p. 971

Zheng, H. Y., Qian, H. X., Zhou, W., 2008. Analyses of surface coloration on TiO_2 film irradiated with excimer laser, Applied Surface Science 254, p. 2174